Self-Assembling Modular Robots Enabled by an Articulated Multi-Axis Connector

Chenghao Xu

Problem Statement

Autonomous modular robots are limited in individual capability and require connector mechanisms tolerating positional and angular misalignment.

Research Goal

Design and evaluate novel connector mechanisms that facilitate reliable autonomous self-assembly, targeting a soft robotic application.

Graphical Abstract

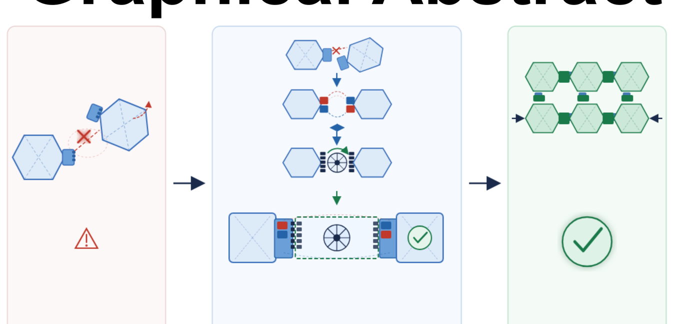

Methodology

- Module Development
- Connector Development
  - Connector Prototype 1
  - Connector Prototype 2
  - Connector Prototype 3
- Data Analysis & Competitor Analysis
- System Validation & Refinement

Background

- Modular robots are robots built from identical modules that connect and disconnect to reconfigure into different shapes.

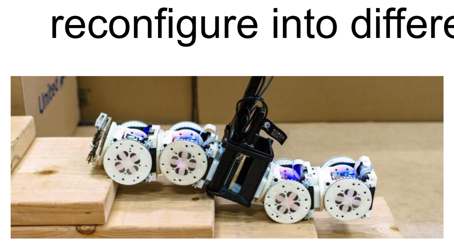

Figure 1: Underwood, 2020

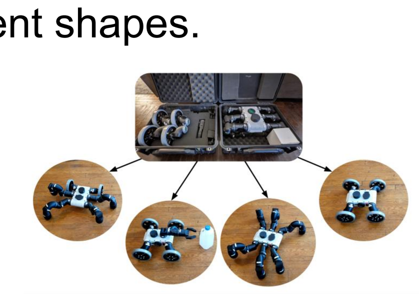

Figure 2: Carnegie Mellon University Robotics Institute

- Magnetic Coupling:
  - Advantage: Errors in alignment
  - Disadvantage: Weak connect force
- Mechanical Coupling:
  - Strong connecting force
  - Requires precise aligning
- Multi-stage coupling mechanisms combine advantages of purely magnetic and mechanical
- Soft robots are deformable and can allow adaptive locomotion, a key advantage over many current modular robots.
- Soft and swarm robotic integration can provide key insights into the real-world application of self-assembly.

Mechanical Designs

Coupling Mechanisms

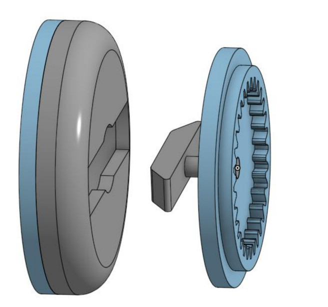

Prototype 1: Key Slot Connector

Uses a protruding key that slides into a matching slot. *Strengths:* provides a strong, rigid connection and is simple to manufacture. *Weaknesses:* gendered design requires specific orientation; alignment tolerance is poor, making docking difficult.

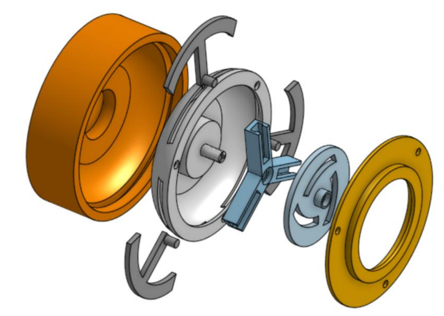

Prototype 2: Gendered Twist-Lock Connector

A bayonet or quarter-turn mechanism inspired by androgynous fasteners. *Strengths:* high versatility, high reliability, low orientation reliance. *Weaknesses:* requires rotation during engagement; can be hard to align under load

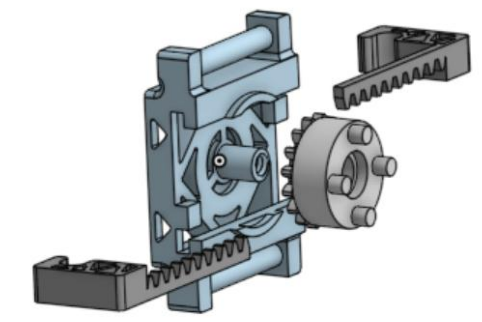

Prototype 3: Rack and Pinion Arm Grabber

A rack-and-pinion mechanism containing an arrangement where a rotating pinion gear meshes with a linear rack to convert rotation into controlled linear motion. *Strengths:* high strength, reversible engagement. *Weaknesses:* requires a certain extent of orientation reliance

Multi-axis Joint

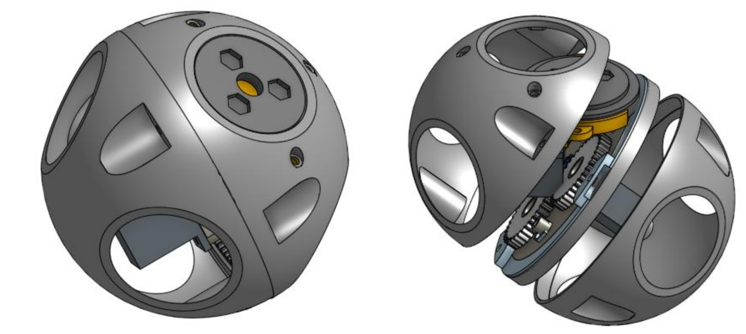

Spherical Connector Joint

The round component is a bio-inspired multi-axis joint. Mimicking human shoulder movement, the ball-and-socket joint allows rotation about multiple axes from a single point. Connectors mounted on this joint can pivot freely in pitch, yaw, and roll, enabling modules to orient themselves for docking in any direction.

Decision Matrix

System	Alignment	Strength	Reverse	Simplicity	Scale	Cost
SMORES-EP	6	9	9	3	6	4
M-Blocks	4	5	8	4	7	3
Truss Links	2	3	2	5	3	5
Soft Mech Connector	8	4	9	7	8	9
Prototype 1	6	6	3	4	6	10
Prototype 2	7	7	5	5	3	10
Prototype 3	8	10	9	6	4	10

Figure 7: Decision matrix comparing modular robotic connector systems and proposed prototypes across six engineering criteria. SMORES-EP, M-Blocks, Truss Links, and a Soft Magnetic Connector were scored on a 1–10 scale (higher = better). Darker cells indicate stronger relative performance.

Finite Element Analysis Simulation

Von Mises Theory

Yielding begins when the **distortional energy per unit volume** equals that of a uniaxial tensile test at yield.

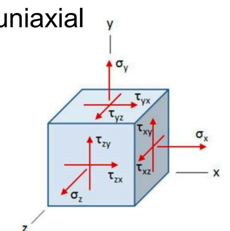

$$\sigma_{vm} = \sqrt{0.5\left[(\sigma_x-\sigma_y)^2+(\sigma_y-\sigma_z)^2+(\sigma_z-\sigma_x)^2\right]+3\left(\tau_{xy}^2+\tau_{yz}^2+\tau_{zx}^2\right)}$$

where σ_x, σ_y, and σ_z are the normal stress values acting in the x, y, and z faces and τ_x, τ_y, and τ_z are the sheer stress values acting in the x, y, and z faces (Patel et al., 2019).

Finite element analysis numerically solves stress and deformation under applied loads, with von Mises stress serving as a failure-predictive metric for ductile materials.

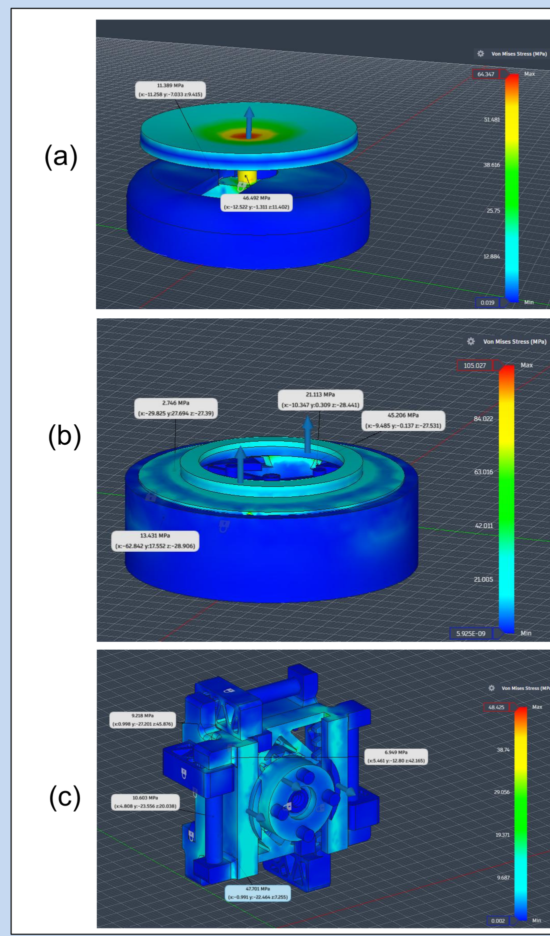

Figure 3: Finite element simulation of the connector under tensile load. The heatmap displays von Mises stress, highlighting peak stresses near the latch and reduced stress in the soft funnel. Simulating with ABS Plastic with ~45 MPa of tensile force (ASTM International), connectors were tested until the breaking point. Stresses remain below material yield limits, validating structural integrity. (a) Prototype 1 withstood ~600 N of force before failure. (b) Prototype 2 withstood ~1.2 kN of force before failure. (c) Prototype 3 withstood ~4.8 kN of force before failure.

Alignment Performance

Success Probability 3D Surfaces

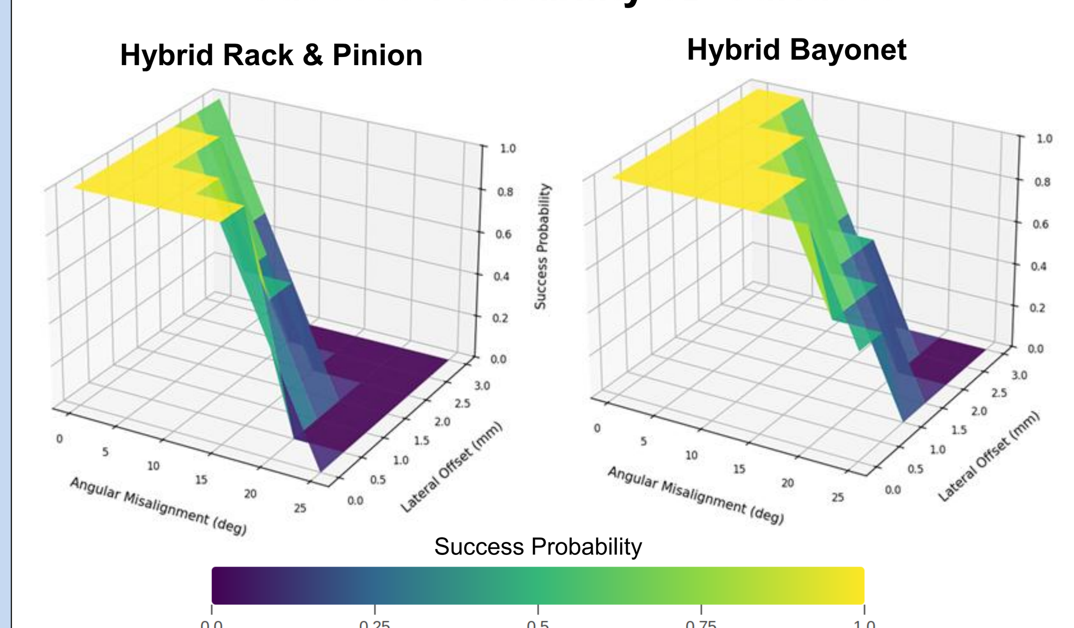

Figure 4: Success probability surfaces for the Hybrid Rack-and-Pinion (left) and Hybrid Bayonet (right) connectors as functions of angular misalignment (degrees) and lateral offset (mm). Both maintain high success at low misalignment, followed by sharp decline beyond critical thresholds. The Bayonet design shows greater tolerance, while the Rack-and-Pinion degrades earlier.

Analysis

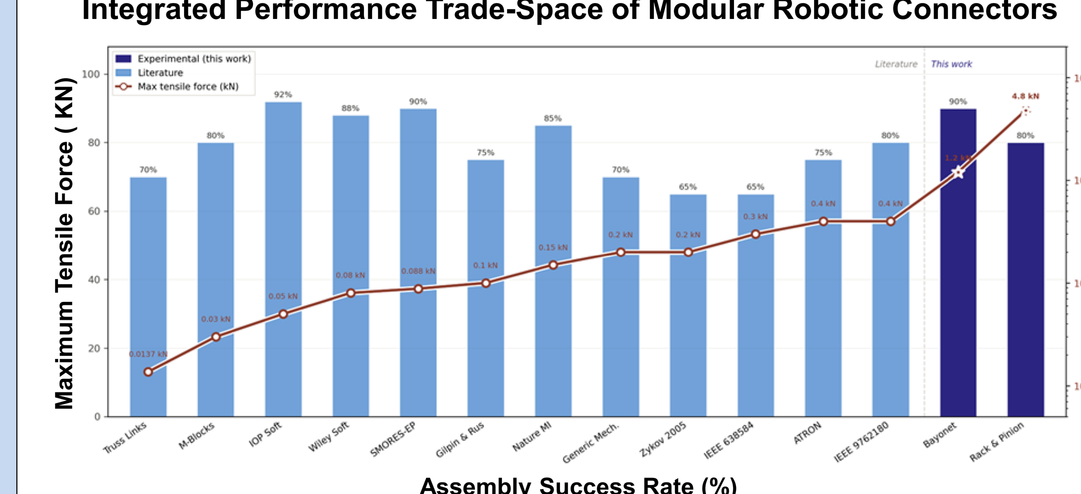

Figure 8: Assembly success rate (%) and maximum tensile force (kN, log scale) are compared across literature and proposed connector designs to illustrate the trade-off between alignment robustness and load-bearing performance.

- The data shows no consistent correlation between tensile strength and assembly success, indicating largely independent performance metrics.
- Prior systems cluster in a moderate-success, low-strength regime, reflecting a persistent limitation in connector design.

Assembly Configurations

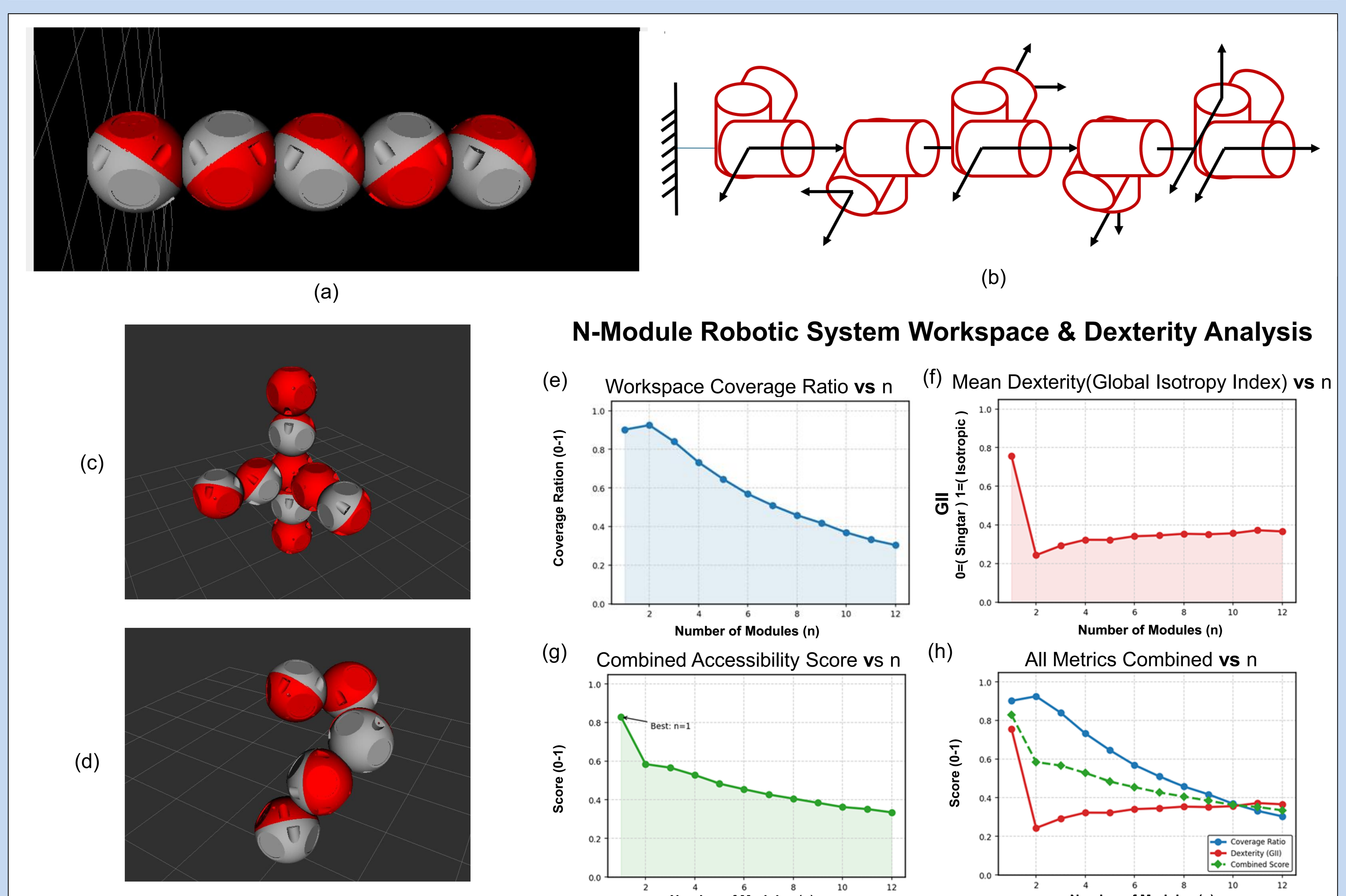

Figure 5: Assembly configurations and workspace analysis of the N-module robotic system. (a) Linear chain of five docked modules. (b) Schematic of N-module assembly sequences. (c–d) Radial and branched 3D configurations demonstrating reconfigurability. (e–g) Workspace coverage, dexterity (GII), and combined accessibility all decline with increasing module count n.

Alignment Algorithm

Navigation & Pose Acquisition

- Free navigation → approach position
- Edge Impulse ML inference

Pose Acquired?
yes → proceed to planning
no → re-center on marker

- Determine marker-centering position

Path Planning & Control

- Arc path planning

PID Controller

$u(t) = K_p \cdot e(t) + K_i \int e(t)\,dt + K_d\, de/dt$

$e(t) = r(t) - y(t)$

- Reference trajectory r(t)

Motion Execution

- Soft body deformation

Arc Segment

$s = r \cdot \theta$ (arc length)

$\kappa = 1/r$ (curvature)

$\theta = \omega \cdot t$ (rotation)

ω = angular velocity

- Execute planned course

Verification & Completion

- Save visual pose to DB
- Log pose estimate

Error Condition

$\|e\| < \varepsilon$ → aligned ✓

$\|e\| \geq \varepsilon$ → re-infer

ε = alignment threshold

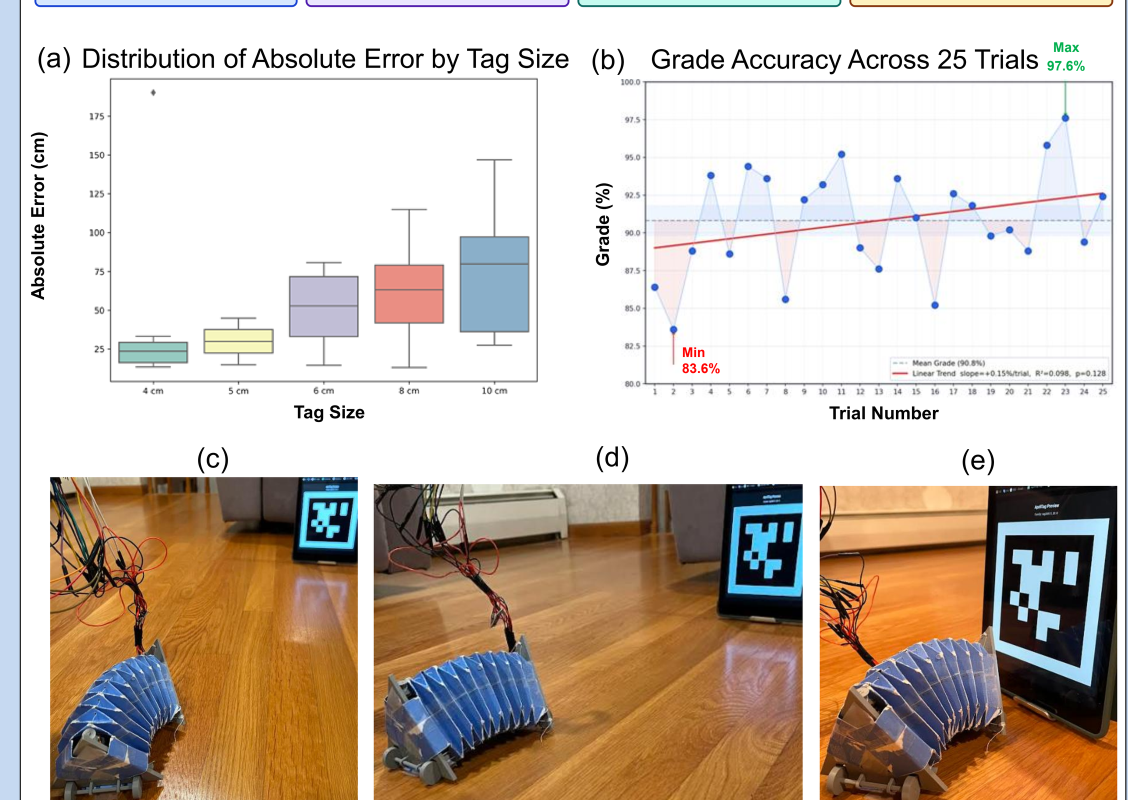

Figure 6: (a) Accuracy vs trial number for 25 trials of autonomous AprilTag alignment. (b) AprilTag pose estimation accuracy for different tag sizes (c) Alignment at t=2 seconds. (d) Alignment at t=6 seconds. (e) Module aligning and achieving a distance ~2.8 cm away.

Conclusions

- **Prototype 3 achieved the strongest overall performance balance**, driven by high load-bearing capacity, strong reversibility, and low projected manufacturing cost
- Hybrid magnetic–mechanical designs outperform purely magnetic or rigid approaches by combining misalignment tolerance with high strength
- Compared to existing **state-of-the-art** systems, the proposed designs exhibit improved scalability and projected **cost efficiency**, indicating feasibility for larger **multi-module** assemblies

Future Work

- Investigate **material substitutions** and fabrication methods to further reduce cost while maintaining mechanical performance.
- Evaluate **repeatability** and **wear behavior** over extended connection cycles to assess long-term reliability and maintenance requirements.
- Optimize maximum allowable angular and translational offsets under which reliable connection can be achieved.

Selected References

ASTM International. *ASTM D638–23:* Standard test method for tensile properties of plastics. ASTM International. https://www.astm.org/d0638

Carnegie Mellon University Robotics Institute. (n.d.). *Modular robots: Mechanism and control design*. Carnegie Mellon University. https://www.ri.cmu.edu/project/modular-robots-mechanism-and-control-design/

Liu, C., Lin, Q., Kim, H., & Yim, M. (2023). SMORES-EP, a modular robot with parallel self-assembly. *Autonomous Robots*, *47*(2), 211–228. https://doi.org/10.1007/s10514-022-10078-1

Patel, R., Riveros, G., Thompson, D., Perkins, E., Hoover, J. J., Peters, J., & Tordesillas, A. (2019). A transdisciplinary approach for analyzing stress flow patterns in biostructures. Mathematical and Computational Applications, *24*(2), 47. https://doi.org/10.3390/mca24020047

Romanishin, J. W., Gilpin, K., Claici, S., & Rus, D. (2015). 3D M-Blocks: Self-reconfiguring robots capable of locomotion via pivoting in three dimensions. *2015 IEEE International Conference on Robotics and Automation (ICRA)*, 1925–1932. https://doi.org/10.1109/ICRA.2015.7139450

Sun, Y., Jiang, Y., Yang, H., Walter, L.-C., Santoso, J., Skorina, E. H., & Onal, C. (2020). Salamanderbot: A soft-rigid composite continuum mobile robot to traverse complex environments. *2020 IEEE International Conference on Robotics and Automation (ICRA)*, 2953–2959. https://doi.org/10.1109/ICRA40945.2020.9196790

Tse, Y. A., Liu, S., Yang, Y., & Wang, M. Y. (2020). A Flexible Connector for Soft Modular Robots Based on Micropatterned Intersurface Jamming. *2020 3rd IEEE International Conference on Soft Robotics (RoboSoft)*, 150–155. https://doi.org/10.1109/RoboSoft48309.2020.9115975

Underwood, E. (2020). *The robots that assemble themselves*. Knowable Magazine. https://knowablemagazine.org/content/article/technology/2020/modular-reconfigurable-robots

Wyder, P. M., Bakhda, R., Zhao, M., Booth, Q. A., Modi, M. E., Song, A., Kang, S., Wu, J., Patel, P., Kasumi, R. T., Yi, D., Garg, N. N., Jhunjhunwala, P., Bhutoria, S., Tong, E. H., Hu, Y., Goldfeder, J., Mustel, O., Kim, D., & Lipson, H. (2025). Robot metabolism: Toward machines that can grow by consuming other machines. *Science Advances*, *11*(29). https://doi.org/10.1126/sciadv.adu6897